

## *In vitro* and *in silico* studies of the inhibitory effects of some novel kojic acid derivatives on tyrosinase enzyme

Azizeh Asadzadeh <sup>1</sup>, Hajar Sirous <sup>2</sup>, Morteza Pourfarzam <sup>2</sup>, Parichehreh Yaghmaei <sup>1</sup>, Afshin Fassihi <sup>3\*</sup>

<sup>1</sup> Department of Biology, Science and Research Branch, Islamic Azad University, Tehran, Iran

<sup>2</sup> Department of Medicinal Chemistry, School of Pharmacy and Pharmaceutical Sciences, Isfahan University of Medical Sciences, Isfahan, Iran

<sup>3</sup> Department of Biochemistry, School of Pharmacy and Pharmaceutical Sciences, Isfahan University of Medical Sciences, Isfahan, Iran

### ARTICLE INFO

#### Article type:

Original article

#### Article history:

Received: Jul 7, 2015

Accepted: Oct 8, 2015

#### Keywords:

Antioxidant activity

*In silico* studies

Kojic acid

Tyrosinase

### ABSTRACT

**Objective(s):** Tyrosinase is a key enzyme in pigment synthesis. Overproduction of melanin in parts of the skin results in hyperpigmentation diseases. This enzyme is also responsible for the enzymatic browning in fruits and vegetables. Thus, its inhibitors are of great importance in the medical, cosmetic and agricultural fields.

**Materials and Methods:** A series of twelve kojic acid derivatives were designed to be evaluated as tyrosinase activity inhibitors. The potential inhibitory activity of these compounds was investigated *in silico* using molecular docking simulation method. Four compounds with a range of predicted tyrosinase inhibitory activities were prepared and their inhibitory effect on tyrosinase activity was evaluated. The antioxidant properties of these compounds were also investigated by *in vitro* DPPH (2,2-diphenyl-1-picrylhydrazyl) and hydrogen peroxide scavenging assays.

**Results:** Compound **IIIId** exhibited the highest tyrosinase inhibitory activity with an IC<sub>50</sub> value of 0.216 ± 0.009 mM which was in accordance with the *in silico* ΔG<sub>bind</sub> results (-13.24 Kcal/mol).

**Conclusion:** Based on the docking studies, from the twelve compounds studied, one (**IIIId**) appeared to have the highest inhibition on tyrosinase activity. This was confirmed by enzyme activity measurements. Compound **IIIId** has an NO<sub>2</sub> group which binds to both of Cu<sup>2+</sup> ions located inside the active site of the enzyme. This compound appeared to be even stronger than kojic acid in inhibiting tyrosinase activity. The DPPH free radical scavenging ability of all the studied compounds was more than that of BHT. However, they were not as strong as BHT or gallic acid in scavenging hydrogen peroxide.

#### ► Please cite this paper as:

Asadzadeh A, Pourfarzam M, Yaghmaei P, Fassihi A. *In vitro* and *in silico* studies of the inhibitory effects of some novel kojic acid derivatives on tyrosinase enzyme. Iran J Basic Med Sci 2016; 19:132-144.

### Introduction

Melanin is produced by a combination of two enzymatic and chemical reactions and protects the skin from the effects of UV sunlight (1, 2). Although melanin plays a crucial protective role against the photo damage of skin, overproduction of this pigment in parts of the skin results in hyper-pigmentation diseases. Tyrosinase catalyzes two key reactions in mammalian melanogenesis. This enzyme is also responsible for the enzymatic browning in fruits and vegetables. Browning in crops is unfavorable and decreases the commercial value of the products (1-3). Tyrosinase is also associated with the host defense, wound healing, molting and sclerotisation of insects (4, 5). Inhibition of this enzyme has become increasingly important for the scientists in clinical, medicinal and cosmetic research. Tyrosinase has always been an important target in food

industry as well. Furthermore, tyrosinase inhibitors have been used as insecticides and insect control agents for years (4).

Although plenty of tyrosinase inhibitors derived from both natural and synthetic sources have been investigated to date, due to off-flavors, food safety, and economic feasibility most have shown insufficient activity and only very few inhibitors are used in the industry (6).

Tyrosinase is a member of a group of metallo-proteins with two copper atoms in the active site. Its functions include monooxygenase (cresolase) and diphenolase (catecholase) activities (7). In the monooxygenase reaction, this enzyme catalyzes the *ortho*-hydroxylation of tyrosine, while in the diphenolase reaction, the *ortho*-dihydroxy compound produced in the monooxygenase reaction is oxidized

\*Corresponding author: Afshin Fassihi. Department of Medicinal Chemistry, School of Pharmacy and Pharmaceutical Sciences, Isfahan University of Medical Sciences, Isfahan, Iran. Tel: +98-313-7922562; Fax: +98-313-6680011; email: fassihi@pharm.mui.ac.ir

to an *ortho*-quinone. Both reactions require molecular oxygen (7-8).

The most intensively studied inhibitor of tyrosinase, kojic acid (5-hydroxy-2-hydroxymethyl-4*H*-pyran-4-one, KA), was discovered by Saito in 1907 and is produced by various fungi (9). KA chelates transition metal ions such as Cu<sup>2+</sup> and Fe<sup>3+</sup> and is an effective free radical scavenger (10). This inhibitor is currently applied as a food additive to prevent enzymatic browning of fruits. KA is also added to cosmeceuticals such as skin-lightening agents. It inhibits both the cresolase and catecholase activity of mushroom tyrosinase. However, its use has been limited because of its cytotoxicity, the skin irritation caused by its use in cosmetics and its instability during storage (9-12). Therefore, the development of novel, potent, non-toxic and stable tyrosinase inhibitors is of great importance in the medical, cosmetic and agricultural fields.

Many semi-synthetic kojic acid derivatives have been synthesized by modifying the structure to improve its pharmacokinetic properties and chelating abilities. Kojyl thioether derivatives have been shown to strongly inhibit the tyrosinase activity (13).

According to Noh *et al* kojic acid-tripeptide amide derivatives exhibited higher storage stability than that of kojic acid (14). In addition, kojic acid derivatives with two pyrone rings have shown eight times more tyrosinase inhibitory potency than kojic acid (15). Of the same scaffold as kojic acid, maltol (3-hydroxy-4*H*-pyran-4-one) and its derivatives have many common biological effects. Inhibitory activity and antioxidant effects of ester derivatives of allomaltol (5-hydroxy-2-methyl-4*H*-pyran-4-one) have been described by Wempe and others (16). Kojic acid has been reported to have antioxidant activity as well. It was reported that the local application of kojic acid accelerates wound healing in rats. This is attributed to the antioxidant activity of KA (17). Some novel 3-hydroxypyridine-4-one derivatives with high antioxidant and iron chelating activity have been synthesized by Mohammadpour and others (18). According to Ahn *et al* the kojic acid derivative containing a trolox moiety, exhibited potent tyrosinase inhibitory and radical scavenging activity (19). KA esters derived from esterification of kojic acid and palm oil based fatty acid also show antioxidant activity (20). Chemical structure of some kojic acid and maltol derivatives as tyrosinase inhibitors are shown in Figure 1. Docking technique is the search over many possible interactions between a ligand and a receptor molecule in order to identify a set of ligand poses that represent local minimum-energy positions of the ligand. This method accurately predicts the structure of a ligand-receptor complex with respect to experiment and calculates a binding energy that can be used to

accurately rank-order different ligands relative to experimentally measured binding affinities. Thus, this method is very informative to clarify key structural characteristics and interactions to provide helpful data for proposing effective receptor inhibitors (21, 22).

In this study, a series of twelve kojic acid derivatives were designed to be evaluated as tyrosinase activity inhibitors. The structural features of some tyrosinase inhibitors reported previously by this group were considered in the design of these compounds (23). To decrease the complications related to wet-lab procedures, the potential inhibitory activity of these compounds was investigated *in silico* using molecular docking simulation method. The most potent predicted compound and also three other compounds which were expected to be moderate to weak inhibitors were prepared and their inhibitory effect on tyrosinase enzyme activity was evaluated. The antioxidant properties of these compounds were also investigated by *in vitro* DPPH (2, 2-diphenyl-1-picrylhydrazyl) and hydrogen peroxide scavenging assays.

## Materials and Methods

### *In silico* studies

For the *in silico* protein-ligand docking simulation, AutoDock4.2 software package was used (24). Lamarckian Genetic Algorithm of the AutoDock 4.2 program was used to perform the flexible-ligand docking studies (25). An Intel-based core i5 personal computer with Linux (redhat 6) operating system was employed for docking procedure. The crystal structure of tyrosinase from *Agaricus bisporus* (AbTYR; PDB code, 2Y9X) was chosen as the protein model for the present study.

### Ligand structure preparation

General structure and the structural details of the compounds subjected to molecular docking simulations are provided in Table 1. All 2D structures of compounds were built using ChemDraw program (ChemDraw Ultra 10.0, Cambridge soft.), then were transferred into Hyperchem 8.0 software (HyperChem, Release 8.0 for Windows, Molecular Modeling System: HyperCube, 2007) and energy minimized with MM<sup>+</sup> force field using Polak-Ribiere conjugate gradient algorithm until the root mean square gradient of 0.01 Kcal/Å.mol. These optimized structures were used as inputs of the AutoDock tools. Then the partial charges of atoms were calculated using the Gasteiger-Marsili procedure implemented in the AutoDock tools package (26). Non-polar hydrogens of compounds were merged and then rotatable bonds were assigned.

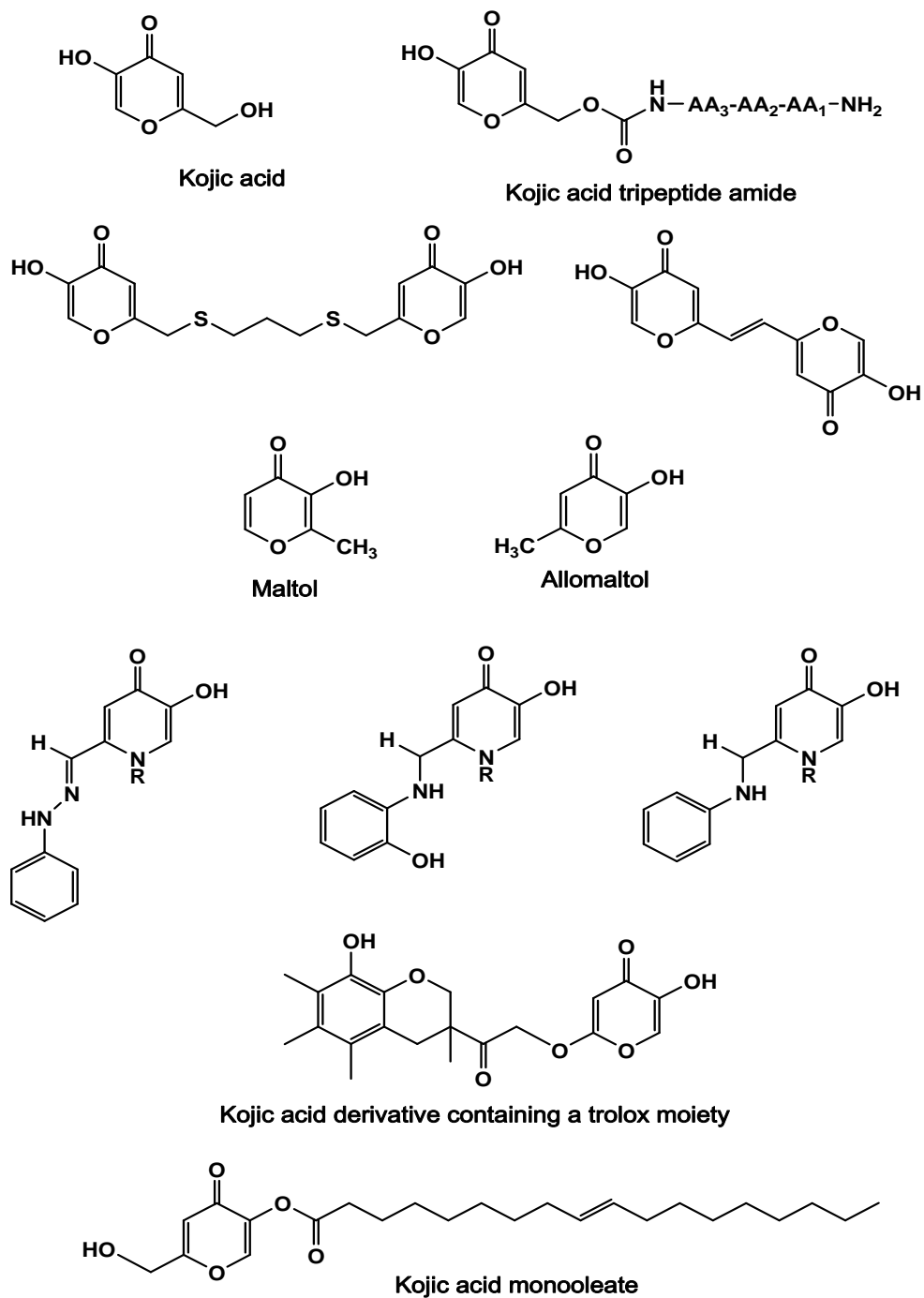
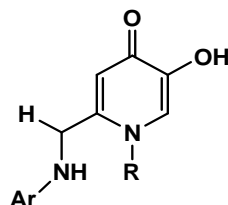


Figure 1. Chemical structure of some synthetic Kojic acid derivatives as tyrosinase inhibitors

**Table 1.** General structures and structural details of the studied compounds

Compound	Ar	R	Mol. Formula	Mol. Weight
1	<i>p</i> -CH <sub>3</sub> C <sub>6</sub> H <sub>4</sub>	CH <sub>3</sub>	C <sub>14</sub> H <sub>16</sub> N <sub>2</sub> O <sub>2</sub>	244.29
2	<i>p</i> -CH <sub>3</sub> OC <sub>6</sub> H <sub>4</sub>	CH <sub>3</sub>	C <sub>14</sub> H <sub>16</sub> N <sub>2</sub> O <sub>3</sub>	260.29
3	<i>p</i> -HOC <sub>6</sub> H <sub>4</sub>	CH <sub>3</sub>	C <sub>13</sub> H <sub>14</sub> N <sub>2</sub> O <sub>3</sub>	246.26
4	<i>o</i> -BrC <sub>6</sub> H <sub>4</sub>	CH <sub>3</sub>	C <sub>13</sub> H <sub>13</sub> BrN <sub>2</sub> O <sub>2</sub>	309.16
5	<i>p</i> -BrC <sub>6</sub> H <sub>4</sub>	CH <sub>3</sub>	C <sub>13</sub> H <sub>13</sub> BrN <sub>2</sub> O <sub>2</sub>	309.16
6	<i>p</i> -CH <sub>3</sub> C <sub>6</sub> H <sub>4</sub>	H	C <sub>13</sub> H <sub>14</sub> N <sub>2</sub> O <sub>2</sub>	230.26
7	<i>p</i> -CH <sub>3</sub> OC <sub>6</sub> H <sub>4</sub>	H	C <sub>13</sub> H <sub>14</sub> N <sub>2</sub> O <sub>3</sub>	246.26
8	<i>o</i> -ClC <sub>6</sub> H <sub>4</sub>	H	C <sub>12</sub> H <sub>11</sub> ClN <sub>2</sub> O <sub>2</sub>	250.68
9	<i>m</i> -ClC <sub>6</sub> H <sub>4</sub>	H	C <sub>12</sub> H <sub>11</sub> ClN <sub>2</sub> O <sub>2</sub>	250.68
10	<i>p</i> -CH <sub>3</sub> CONHC <sub>6</sub> H <sub>4</sub>	H	C <sub>14</sub> H <sub>15</sub> N <sub>3</sub> O <sub>3</sub>	273.29
11	<i>m</i> -NO <sub>2</sub> C <sub>6</sub> H <sub>4</sub>	H	C <sub>12</sub> H <sub>11</sub> N <sub>3</sub> O <sub>4</sub>	261.23
12	4-C <sub>5</sub> H <sub>4</sub> N	H	C <sub>11</sub> H <sub>11</sub> N <sub>3</sub> O <sub>2</sub>	217.22

### Protein structure preparation

A tyrosinase from the mushroom *A. bisporus* has been successfully crystallized by Wangsa Ismaya and its structure has been elucidated by means of X-ray crystallography. The enzyme is commonly found as a H<sub>2</sub>L<sub>2</sub> tetramer. The H subunit is the tyrosinase domain with a molecular mass of 43 kDa. This subunit contains two copper atoms coordinated by six histidine residues, His85, His61, His94, His259, His263 and His296. The L subunit is 14 kDa with a lectin-like fold and the function of this subunit is unknown. This tetramer is stabilized by two holmium ions in the H-H interface (27).

Co-crystallized ligands (tropolone), all chains except chain A, two holmium ions and water molecules of crystallization were removed from the complex using

Discovery StudioVisualizer (28). All missing hydrogens were added and after determining the Kolman united atom charges, non-polar hydrogens were merged to their corresponding carbons using Autodock tools (29).

### Docking procedure

The AutoGrid program performs pre-calculations for the docking of a ligand to a set of grids that describe the effect that the protein has on point charges. The effect of these forces on the ligand is then analyzed by the AutoDock program. Using Autogrid as a part of the Auto dock package, desolvation parameters and electrostatic interactions were assigned to each protein atom. In all dockings, a grid map of 40 × 40 × 40 points and a grid point spacing of 0.375 Å (a quarter of the C-C bond) were applied using Autogrid software. The grid

center was placed between the two metal ions located in the active site. The Lamarckian Genetic Algorithm (LGA) approach was selected as the search algorithm for the global optimum binding position search among the three different search algorithms offered by AutoDock 4.2. This algorithm has been determined superior compared with simulated annealing and genetic algorithm. 100 independent docking runs were carried out for each ligand. For the LGA method, an initial population of random individuals with a population size of 150 individuals, a maximum number of energy evaluations:  $2.5 \times 10^6$  per run, a maximum number of generations of 27000, an elitism value of 1, a mutation rate of 0.02, and a crossover rate of 0.8 were used. All other run parameters were maintained at their default settings. At the end of docking, the structures were ranked by energy, as were the clusters and binding free energy of each run was provided in the docking log (dlg) file. The resulting docking poses were analyzed in AutoDockTools and DS Visualizer 3.5 and Ligplot softwares (30).

Hydrogen bonding and Pi interactions were established through the docking procedure. The possibility of metal ions coordination within the active site of protein was investigated using the "Bump Monitor" option in DS visualizer 3.5. Bump identifies a close contact between two atoms. The ligand bound protein was used as the input file for LigPlot to generate the two dimensional (2D) plot of the hydrogen bond interaction and also the hydrophobic interactions.

### Chemistry

Chemicals supplied by Merck or Sigma-Aldrich Chemical Co. were used without further purification. Analytical thin-layer chromatography (TLC) was performed using Merck silica gel (60F<sub>254</sub>) plates. Melting points were determined employing a Mettler capillary melting point apparatus and were uncorrected. The infrared (IR) spectra were recorded with a WQF-510 Ratio Recording FT-IR spectrometer as a KBr disc ( $\gamma$ ,  $\text{cm}^{-1}$ ). The <sup>1</sup>H-NMR and <sup>13</sup>C-NMR spectra (DMSO-d<sub>6</sub>) were recorded using a Bruker 400 MHz spectrometer. Chemical shifts ( $\delta$ ) are reported in ppm downfield from the internal standard tetramethylsilane (TMS). Elemental analyses were carried out with a Perkin Elmer Model 240-C apparatus. Elemental microanalyses were within  $\pm 0.4\%$  of the theoretical values for C, H and N. The purity of the compounds was checked by TLC on silica gel plate using chloroform and methanol as solvent.

Compounds selected to be prepared were synthesized starting from one of the two aldehydes: 5-(benzyloxy)-1-methyl-4-oxo-1,4-dihydropyridine-2-carbaldehyde (**1a**) and 5-(benzyloxy)-4-oxo-1,4-dihydropyridine-2-carbaldehyde (**1b**). The methods for the preparation of these aldehydes are reported previously (18). The chemical procedure applied for the

synthesis of compounds **11a-d** (**11a**: **3**, **11b**: **2**, **11c**: **7** and **11d**: **11**) is outlined in Scheme 1 and details are given below.

### General procedure for the preparation of Kojic acid derivatives (11a-d)

A mixture of 1.0 mmol of 5-(benzyloxy)-1-methyl-4-oxo-1,4-dihydropyridine-2-carbaldehyde (**1a**) or 5-(benzyloxy)-4-oxo-1,4-dihydropyridine-2-carbaldehyde (**1b**) and 1.0 mmol of the appropriately substituted aniline in 5 mL of CHCl<sub>3</sub>:EtOH (8:2), as solvent, was reacted under reflux condition. The progress of the reaction was monitored by TLC using n-hexane:ethylacetate (3:1) as solvent. After the completion of the reaction, solvent was removed by rotary evaporation and the final product was purified by recrystallization in absolute ethanol or ethylacetate. 1.0 mmol of the obtained product was dissolved in 5 mL of absolute ethanol. Hydrogenation process was performed under constant pressure of H<sub>2</sub> over 10 wt% of Pd/C as catalyst at room temperature. The progress of the reaction was followed by TLC using n-hexane:ethylacetate (3:1) as solvent. After the completion of the reaction, the reaction mixture was heated up to the boiling point and filtered through a sintered glass while hot. The filtrate was then evaporated to dryness to obtain the deprotected hydroxyl derivatives (**11a-d**) which were further purified by recrystallization in hot ethanol. The spectral details of the prepared compounds are provided in the results section.

### Biological assay

#### Tyrosinase inhibition assay

Tyrosinase activity inhibition was determined as described by Iida and coworkers (31), with the following modifications. L-dopa and mushroom tyrosinase (EC 1.14.18.1) were purchased from Sigma-Aldrich (St. Louis, MO, USA). The UV/VIS spectra were recorded with a Perkin Elmer U/Vis spectrophotometer. Briefly, 450  $\mu\text{l}$  of phosphate buffer (50 mM, pH 6.5), 20  $\mu\text{l}$  of mushroom tyrosinase (2800 U/mL) in phosphate buffer and 340  $\mu\text{L}$  of the inhibitor solution were placed in a cuvette. After pre-incubation for 8 min at 25 °C, 200  $\mu\text{l}$  of L-DOPA (4.25 mM) was added and the cuvette was further incubated at 25 °C for 10 min. Subsequently the absorbance of dopa-chrome formed was measured at 475 nm. Kojic acid and phosphate buffer were used instead of the inhibitor solution as positive and negative tyrosinase inhibitor control, respectively. The extent of the inhibition by the test compound was expressed as the percentage of concentration necessary to achieve 50% inhibition (IC<sub>50</sub>). The percentage of tyrosinase inhibition was calculated as follows:

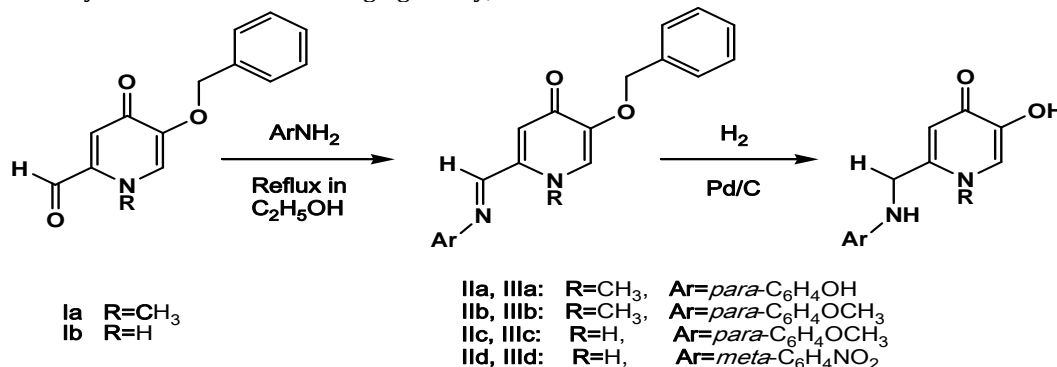
$$\text{Inhibitory activity (\%)} = [(A_c - A_t) / A_c] \times 100$$

where, A<sub>c</sub> is the absorbance of the negative control and A<sub>t</sub> is the absorbance of the test compound.

**Antioxidant evaluation****DPPH free radical scavenging assay**

The antioxidant activity of the studied compounds was evaluated by DPPH radical scavenging assay,

originally described by Blois and coworkers (32). In brief, a stock solution of DPPH (60  $\mu$ M) was prepared in methanol and 1 ml of this stock solution was added to 1 ml of the standard and test solution at different



**Scheme 1.** General procedures applied for the synthesis of the studied compounds

**Table 2.** Docking results of Kojic acid derivatives docked into tyrosinase active site. The values are expressed in kcal/mol

Compound	$\Delta G_{\text{bind}}$	Intermolecular Energy	Electrostatic Energy
1	-2.39	-3.49	-1.42
2 <sup>a</sup>	-2.33	-3.70	-1.04
3 <sup>a</sup>	-2.47	-3.84	-0.78
4	-2.79	-3.89	-1.54
5	-2.3	-3.4	-1.39
6	-2.63	-3.73	-1.97
7 <sup>a</sup>	-2.25	-3.62	-0.71
8	-3.08	-4.18	-2.05
9	-3.11	-4.21	-1.96
10	-3.51	-4.88	-1.74
11 <sup>a</sup>	-13.24	-14.61	-13.31
12	-2.69	-3.52	-1.66
Tropolone	-3.11	-3.38	-1.51

<sup>a</sup>3: IIIa, 2: IIIb, 7: IIIc and 11: IIIId

**Table 3.** Interactions between the studied compounds and the active site residues of tyrosinase

Compound	Interaction with Cu <sup>2+</sup>	Interaction with amino acid residues		
		H-bonding	Pi interactions	Hydrophobic
1	C=O... Cu <sup>2+</sup> (2.523)	His <sub>263</sub>	His <sub>263</sub> (sigma- $\pi$ )	Gly <sub>281</sub> , Asn <sub>260</sub> , His <sub>85</sub> , Val <sub>283</sub> , Ser <sub>282</sub> , His <sub>61</sub> , His <sub>259</sub>
2 <sup>a</sup>	C=O... Cu <sup>2+</sup> (2.430)	Asn <sub>260</sub>	His <sub>263</sub> (sigma- $\pi$ )	His <sub>263</sub> , Phe <sub>264</sub> , Ala <sub>286</sub> His <sub>85</sub> , His <sub>244</sub> , Val <sub>283</sub> , His <sub>61</sub> , His <sub>259</sub> , His <sub>263</sub> , Phe <sub>292</sub> , Ala <sub>286</sub> , Glu <sub>322</sub>
3 <sup>a</sup>	C=O... Cu <sup>2+</sup> (2.521) <sup>b</sup>	His <sub>263</sub>	His <sub>263</sub> (sigma- $\pi$ )	Gly <sub>281</sub> , Met <sub>280</sub> , Asn <sub>260</sub> , His <sub>85</sub> , His <sub>244</sub> , Phe <sub>264</sub> , Val <sub>283</sub> , Ser <sub>282</sub> , His <sub>61</sub> , His <sub>259</sub> , His <sub>263</sub> , Ala <sub>286</sub>
4	C=O... Cu <sup>2+</sup> (2.367)	His <sub>263</sub>	His <sub>263</sub> (sigma- $\pi$ )	Gly <sub>281</sub> Val <sub>283</sub> , Ser <sub>282</sub> , His <sub>61</sub> , His <sub>259</sub> , His <sub>263</sub> , Phe <sub>264</sub> , Ala <sub>286</sub> , Met <sub>280</sub>
5	C=O... Cu <sup>2+</sup> (2.523)	His <sub>263</sub> , His <sub>259</sub>	-	Gly <sub>281</sub> , Asn <sub>260</sub> , His <sub>85</sub> , His <sub>244</sub> , Val <sub>283</sub> , Ser <sub>282</sub> , His <sub>61</sub> , His <sub>259</sub> , His <sub>263</sub> , Phe <sub>264</sub> , Ala <sub>286</sub>
6	C=O... Cu <sup>2+</sup> (2.348) C=O... Cu <sup>2+</sup> (2.324)	Asn <sub>260</sub>	-	Gly <sub>281</sub> , His <sub>85</sub> , Val <sub>283</sub> , His <sub>259</sub> , His <sub>263</sub> , Phe <sub>264</sub> , Ala <sub>286</sub> , Phe <sub>292</sub>
7 <sup>a</sup>	C=O... Cu <sup>2+</sup> (2.213)	Asn <sub>260</sub>	-	Gly <sub>281</sub> , His <sub>85</sub> , Val <sub>283</sub> , Ser <sub>282</sub> , His <sub>61</sub> , His <sub>263</sub> , Phe <sub>264</sub> , Ala <sub>286</sub> , Phe <sub>292</sub>
8	C=O... Cu <sup>2+</sup> (2.130)	His <sub>61</sub> , His <sub>296</sub>	-	Gly <sub>281</sub> , Met <sub>280</sub> , His <sub>85</sub> , Val <sub>283</sub> , Ser <sub>282</sub> , His <sub>259</sub> , His <sub>263</sub> , Phe <sub>264</sub> , Ala <sub>286</sub> , Phe <sub>292</sub> , Phe <sub>90</sub>
9	C=O... Cu <sup>2+</sup> (2.450) C=O... Cu <sup>2+</sup> (2.333)	Asn <sub>260</sub> , His <sub>259</sub> , His <sub>296</sub>	-	Gly <sub>281</sub> , His <sub>85</sub> , Val <sub>283</sub> , Ser <sub>282</sub> , His <sub>61</sub> , His <sub>263</sub> , Phe <sub>264</sub> , Ala <sub>286</sub> , Phe <sub>292</sub>
10	-	His <sub>61</sub> , His <sub>85</sub> , Val <sub>283</sub> , Gly <sub>281</sub>	-	Gly <sub>281</sub> , Asn <sub>260</sub> , Ser <sub>282</sub> , His <sub>259</sub> , His <sub>263</sub> , Ala <sub>286</sub> , Phe <sub>292</sub>
11 <sup>a</sup>	N=O... Cu <sup>2+</sup> (2.255) N=O... Cu <sup>2+</sup> (2.279)	His <sub>259</sub> , Asn <sub>260</sub> His <sub>296</sub> , His <sub>61</sub> His <sub>244</sub> , Glu <sub>256</sub>	-	Gly <sub>281</sub> , His <sub>94</sub> , Val <sub>283</sub> , Ser <sub>282</sub> , His <sub>61</sub> , His <sub>263</sub> , Asn <sub>260</sub> , His <sub>259</sub> , Phe <sub>264</sub> , Phe <sub>90</sub> , Phe <sub>292</sub> , Ala <sub>286</sub>
12	C=O... Cu <sup>2+</sup> (2.344)	-	-	Gly <sub>281</sub> , Met <sub>280</sub> , Asn <sub>260</sub> , Val <sub>283</sub> , Ser <sub>282</sub> , His <sub>61</sub> , His <sub>259</sub> , His <sub>263</sub>

<b>Tropolone</b>	C=O...Cu <sup>2+</sup> (2.519)	His <sub>263</sub> , His <sub>61</sub>	Phe <sub>264</sub> , Phe <sub>292</sub>
		ASN <sub>260</sub>	Gly <sub>281</sub> , His <sub>259</sub> , Val <sub>283</sub> , Ser <sub>282</sub> , His <sub>61</sub> , His <sub>263</sub> , Ala <sub>286</sub> , Met <sub>280</sub>
		His <sub>263</sub>	
		(cation-π) (π-π)	

<sup>a</sup> 3: IIIa, 2: IIIb, 7: IIIc and 11: IIId

<sup>b</sup> The value in parenthesis is the distance between donor atom and Cu<sup>2+</sup> ion expressed in Å

concentrations (0.0125, 0.025, 0.05, 0.1 and 0.2 mg/ml). The mixture was shaken vigorously and allowed to stand for 30 min, and then the absorbance of the resulting solution was measured at 517 nm using a UV/Vis spectrophotometer. The DPPH scavenging activity was calculated as follows:

$$\text{DPPH scavenging activity (\%)} = [(A_c - A_t) / A_c] \times 100$$

where, A<sub>c</sub> is the absorbance of the control tube (containing all reagents except the test compound), and A<sub>t</sub> is the absorbance of the test tube. Butylated hydroxytoluene (BHT) was used as a standard antioxidant.

### Hydrogen peroxide scavenging assay

H<sub>2</sub>O<sub>2</sub> scavenging power of the studied compounds was determined as described by Ruch and coworkers (33). This method is based on the ability of a compound to convert hydrogen peroxide to water. A solution of hydrogen peroxide (40 mM) was prepared in saline phosphate buffer (pH 7.4) and concentrations were determined spectrophotometrically at 230 nm. 100 μl of a methanolic solution of the test compounds or standards (0.312 mg/ml) was added to 2 ml of hydrogen peroxide solution and the absorbance was determined at 230 nm after 20 min against a blank solution containing 100 μl of a methanolic solution of test compounds or standards and 2 mL of saline phosphate buffer. The percentage of hydrogen peroxide scavenging by compounds and standards was calculated using the following equation:

$$\text{H}_2\text{O}_2 \text{ scavenging activity (\%)} = [(A_c - A_t) / A_c] \times 100$$

where, A<sub>c</sub> is the absorbance of the control (containing all reagents except the test compound) and A<sub>t</sub> is the absorbance in the presence of the test compounds or standards. BHT and gallic acid were used as standards.

### Statistical analysis

The IC<sub>50</sub> values for the tyrosinase assay and DPPH scavenging ability were calculated from the logarithmic non-linear regression curve derived from the plotted data using GraphPad Prism Software Version 5.0 (GraphPad Prism Software, San Diego, CA, USA). The data were expressed as mean ± standard deviation of three replicates. The mean values, standard deviation and the inhibition curves were prepared using the EXCEL program from Microsoft Office 2010 package.

## Results

### In silico studies

The results of this part of study including the estimated free binding energy values (ΔG<sub>bind</sub>) of the docked positions, expressed in kcal/mol, and the favorable interactions with key amino acid residues at the active site of enzyme are presented in Tables 2 and 3, respectively.

### Chemistry

The structures of the title compounds were confirmed by FTIR, <sup>1</sup>HNMR and <sup>13</sup>CNMR spectroscopy as well as elemental analysis. Some of the characterization data of the prepared compounds are summarized in Table 4.

The detailed FTIR, <sup>1</sup>HNMR and <sup>13</sup>CNMR spectroscopy results are described below. The carbon atoms of the pyridinone ring are assigned with plain numbers and those of the aromatic substituent at the C-2 position of the main scaffold are given prime (') suffixes.

### 5-Hydroxy-2-[(4-hydroxyphenylamino)methyl]-1-methylpyridin-4(1H)-one (IIIa)

Dark brown powder; FT-IR (KB) cm<sup>-1</sup>: 2500-3500 (O-H, str.), 3228 (N-H, str.), 3072 (C-H, aromatic, str.), 2954 (C-H, aliphatic, str.), 1630 (C=O, str.), 1556 (shouldered, C=C aromatic, C=C alkene), 1516 (C=C, aromatic, bend); <sup>1</sup>HNMR (DMSO-d<sub>6</sub>): δ 8.61 (s, 1H, OH), 7.54 (s, 1H, C-6-H), 6.56 (d, J = 8.80 Hz, 2H, C-3'-H, C-5'-H), 6.48 (d, J = 8.80 Hz, 2H, C-2'-H, C-6'-H), 6.21 (s, 1H, C-3-H), 5.61 (bs, 1H, NH-CH<sub>2</sub>), 3.95 (s, 2H, NH-CH<sub>2</sub>), 3.66 (s, 3H, N-CH<sub>3</sub>); <sup>13</sup>CNMR (DMSO-d<sub>6</sub>): δ 169.66 (C-4), 157.33 (C-5), 150.09 (C-2), 148.74 (C-4'), 140.58 (C-1'), 123.29 (C-6), 115.71 (C-3', C-5'), 115.61 (C-2', C-6'), 113.67 (C-3), 52.79 (CH<sub>2</sub>-NH), 44.05 (CH<sub>3</sub>-N).

### 5-Hydroxy-2-[(4-methoxyphenylamino)methyl]-1-methylpyridin-4(1H)-one (IIIb)

Light brown powder; FT-IR (KB) cm<sup>-1</sup>: 2500-3500 (O-H, str.), 3417 (N-H str.), 3282 (C-H, aromatic, str.), 2833 (C-H, aliphatic, str.), 1639 (C=O, str.), 1564 (shouldered, C=C aromatic, C=C alkene), 1456 (C=C, aromatic, bend); <sup>1</sup>HNMR (DMSO-d<sub>6</sub>): δ 7.43 (s, 1H, C-6-H), 6.73 (d, J = 9.20 Hz, 2H, C-3'-H, C-5'-H), 6.58 (d, J = 9.20 Hz, 2H, C-2'-H, C-6'-H), 6.18 (s, 1H, C-3-H), 5.82 (bs, 1H, NH-CH<sub>2</sub>), 4.17 (s, 2H, NH-CH<sub>2</sub>), 3.66 (s, 3H, O-CH<sub>3</sub>), 3.64 (s, 3H, N-CH<sub>3</sub>); <sup>13</sup>CNMR (DMSO-d<sub>6</sub>): δ 170.28 (C4), 151.06 (C-5), 146.57 (C-2), 146.26 (C-4'), 141.96 (C-1'), 124.41 (C-6), 114.58 (C-3', C-5'), 113.31 (C-2', C-6'), 111.66 (C-3), 55.25 (CH<sub>2</sub>-NH, O-CH<sub>3</sub>), 43.71 (CH<sub>3</sub>-N).

### 5-Hydroxy-2-[(4-methoxyphenylamino)methyl]pyridin-4(1H)-one (IIIc)

Light brown powder; FT-IR (KB) cm<sup>-1</sup>: 2500-3500 (O-H, str.), 3365 (N-H, str.), 3251 (N-H, str.), 3082 (C-H, aromatic, str.), 3030 (C-H, aromatic, str.), 2925 (C-H, aliphatic, str.), 1628 (C=O, str.), 1514 (shouldered, C=C aromatic, C=C alkene, str.), 1483 (C=C, aromatic, bend); <sup>1</sup>HNMR (DMSO-d<sub>6</sub>): δ 11.18 (s, 1H, NH ring), 7.24 (s, 1H, C-6-H), 6.71 (d, J = 8.40 Hz, 2H, C-3'-H, C-5'-H), 6.51 (d, J = 8.40 Hz, 2H, C-2'-H, C-6'-H), 6.12 (s, 1H, C-3-H).

H), 5.83 (bs, 1H, NH-CH<sub>2</sub>), 4.08 (d, J= 4.00 Hz, 2H, NH-CH<sub>2</sub>), 3.62 (s, 3H, O-CH<sub>3</sub>); <sup>13</sup>CNMR (DMSO-d<sub>6</sub>): δ 169.37 (C-4), 157.82 (C-5), 151.27 (C-2), 142.23 (C-4'), 134.12 (C-1'), 122.49 (C-6), 114.55 (C-3', C-5'), 113.52 (C-2', C-6'), 109.79 (C-3), 59.95 (CH<sub>2</sub>-NH), 55.22 (O-CH<sub>3</sub>).

#### 5-Hydroxy-2-[(3-nitrophenylamino)methyl]pyridin-4(1H)-one (III d)

Pale yellow powder; FT-IR (KB) cm<sup>-1</sup>: 2500-3500 (O-H, str.), 3157 (N-H, str.), 3032 (C-H, aromatic, str.), 2922 (C-H, aliphatic, str.), 1620 (C=O, str.), 1541 (shouldered, C=C aromatic, C=C alkene, str.), 1518 (C=C, aromatic, bend); <sup>1</sup>HNMR (DMSO-d<sub>6</sub>): δ 11.79 (s, 1H, O-H), 10.90 (s, 1H, NH ring), 8.36 (s, 1H, C-6-H), 8.13-8.10 (m, 2H, C-2'-H, C-4'-H), 7.71-7.74 (m, 3H, C-5'-H, C-6'-H, C-3-H), 7.36-7.50 (m, 7H, CH<sub>2</sub>-C<sub>6</sub>H<sub>5</sub>), 5.93 (bs, 1H, NH-CH<sub>2</sub>), 4.30 (d, J= 4.00 Hz, 2H, NH-CH<sub>2</sub>); <sup>13</sup>CNMR (DMSO-d<sub>6</sub>): δ 169.68 (C-4), 150.78 (C-1'), 150.08 (C-3'), 148.68 (C-5), 109.69 (C-6), 106.93 (C-3), 59.95 (CH<sub>2</sub>-NH).

#### Biological assay

##### Tyrosinase inhibition assay

The effect of the studied compounds on the activity of mushroom tyrosinase was examined at different concentrations and compared. To compare the inhibitory potencies, kojic acid was employed as a positive control. The results are provided as graphs in Figure 2. The concentrations at which the studied compounds induced a 50% loss in activity (IC<sub>50</sub>) were estimated and are reported in Table 5.

Table 4. Some characterization data of the prepared compounds

Compound	M.P. (°C)	Yield (%)	Analysis (%)		
			Found (Calculated)		
			C	H	N
IIIa	242.5-	89	68.95	6.48	11.54
	243.2		(68.83)	(6.60)	(11.47)
IIIb	254.5-	94	64.44	6.54	10.95
	255.7		(64.60)	(6.20)	(10.76)
IIIc	194.0-	92	63.72	5.66	11.72
	195.5		(63.40)	(5.73)	(11.38)
III d	254.8-	90	54.95	4.33	16.41
	255.2		(55.17)	(4.24)	(16.09)

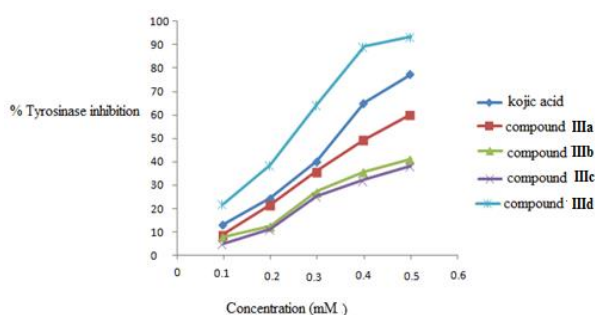


Figure 2. Dose-dependent inhibition of mushroom tyrosinase by Kojic acid derivatives. Tyrosinase activity was measured using L-DOPA as the substrate. Each value represents mean  $\pm$  S.D (n = 3)

#### Antioxidant evaluation

##### DPPH free radical scavenging assay

The IC<sub>50</sub> values for DPPH free radical scavenging ability of methanolic solutions of the studied compounds and positive controls were calculated and are presented in Table 5.

##### Hydrogen peroxide scavenging assay

Results of the scavenging ability of the studied compounds on hydrogen peroxide are presented in Table 5. These values are measured at the concentration of 0.312 mg/ml for the studied compounds and controls. BHT and gallic acid were used as positive controls.

#### Discussion

The binding mode of the studied compounds against tyrosinase was investigated by performing molecular docking studies. There is no X-ray crystallography data available for the three-dimensional structure of human tyrosinase (34). Thus, the 3D structure of *A. bisporus* mushroom tyrosinase was used for the docking study. Possible H-bonding,  $\pi$ -sigma, cation- $\pi$  and metal interactions assessed using the Discovery StudioVisualizer program. Ligplot software predicted the possible hydrophobic interaction between the docked ligands and the catalytic site residues.

Tropolone was redocked into the active site of tyrosinase for the method validation in the first step of docking procedure. The binding energy of the best bound conformation of tropolone was -3.11 kcal/mol. It interacted with HIS263 through  $\pi$ - $\pi$  and cation- $\pi$  interaction and its OH group formed a hydrogen-bond with Asn<sub>260</sub> (Figure 3).

Following the validation of the docking protocol, the 3D structures of the studied compounds were docked into the tyrosinase enzyme. The most and the least active compounds, based on  $\Delta G_{\text{bind}}$ , were selected for further laboratory evaluations. **11**, with  $\Delta G_{\text{bind}} = -13.24$  kcal/mol, predicted as the most potent compound in tyrosinase activity inhibition, and **7** ( $\Delta G_{\text{bind}} = -2.25$  kcal/mol) as the least potent one were subjected to tyrosinase activity inhibition assay. Two other weak compounds, **2** and **3**, were also selected for tyrosinase inhibition assay as well as for antioxidant evaluations. The best docked conformations of tropolone; compounds **IIIa** (**3**), **IIIb** (**2**), **IIIc** (**7**) and **III d** (**11**) in the tyrosinase binding site are shown in Figure 4. This Figure reveals that all the studied compounds occupied the same space as tropolone with a similar binding mode. It can be seen that tropolone and kojic acid derivatives shared common hydrogen bonds with Asn<sub>260</sub> and His<sub>263</sub> residues. The docking results for all

compounds were in accordance with the docking results reported by others in terms of the amino

residues involved in interaction with the inhibitor molecule (34 -38).

**Table 5.** Tyrosinase inhibitory activity of the studied compounds compared with kojic acid, IC<sub>50</sub> values for the 2,2-diphenyl-1-picrylhydrazyl scavenging ability of the studied compounds and Percentage of the H<sub>2</sub>O<sub>2</sub> scavenging activity of the studied compounds. Each value represents mean± SD (n = 3)

Compound	IIIa	IIIb	IIIc	IIId	Kojic acid <sup>a</sup>	BHT	Galic acid
IC <sub>50</sub> values for Tyrosinase inhibitory activity (mM)±SD	0.4037±0.014	0.6172±0.019	0.6569±0.028	0.2169±0.009	0.3194±0.012	NA <sup>b</sup>	NA
IC <sub>50</sub> values for DPPH (µg/ml)±SD	34.38±1.9	44.62±2.9	21.38±1.4	25.17±1.8	NA	49.19±1.7	NA
H <sub>2</sub> O <sub>2</sub> Scavenging (%)±SD	63.70±1.49	64.97±0.96	67.20±1.14	61.77±1.16	NA	78.52±1.85	97.39±0.76

<sup>a</sup> positive control used in the assay

<sup>b</sup>Not analyzed

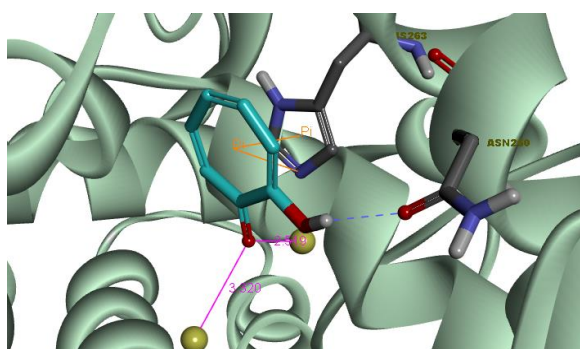


**Figure 3.** Redocking results of tropolone in the active site of tyrosinase. Ligands are represented by a stick model and are colored by elements. The solid ribbon model shows the backbone of tyrosinase catalytic core domain and key interacting amino acid residues are shown as stick models. The metal ions are represented as yellow spheres. Hydrogen bonds are shown by blue dashed line. The possible interaction between metal ions and ligands are marked by violet line and Pi ( $\pi$ ) interactions represented as orange lines

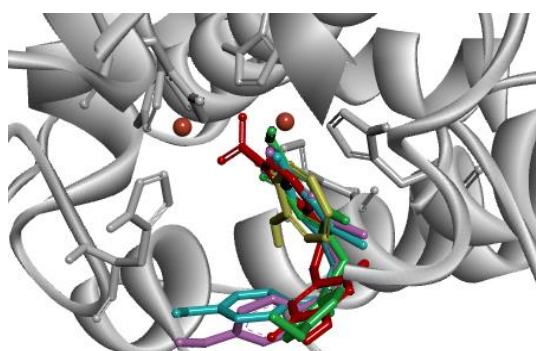


**Figure 4.** Docked conformations of ligand structures in the binding site of tyrosinase. Tropolone (yellow), compound IIIa (cyan), compound IIIb (Magenta), compound IIIc (green) and compound IIId (red) are superimposed in this Figure.

In the case of compound IIIa, an H-bonding and a sigma- $\pi$  interaction through the carbonyl moiety with the imidazole ring of His263 were detected (Figure 5A). The NH moiety of compound IIIb formed a hydrogen bond with Asn260 and interacted with the imidazole ring of His263 by sigma-  $\pi$  interaction through the carbonyl moiety (Figure 5B). Hydrogen bond formation with Asn260 in the tyrosinase active site was also observed in the docked conformation of the compound IIIc (Figure 5C).

Crystallographic data have revealed that tyrosinase active site of *A. bisporus* holds two divalent copper ions that are essential for the formation of a catalytic active complex (27). In this study, docked conformations of compounds IIIa, IIIb and IIIc have shown the possibility of some interaction with one of the copper ions. Due to the appropriate distance (<2.521 Å) between the oxygen atom of the carbonyl moiety and the metal ion, formation of electrostatic interactions is acceptable. among the studied compounds, the best docking result was obtained for compound IIId that showed a high inhibitory potency. In fact, this compound had the most negative  $\Delta G_{\text{bind}}$  (-13.24 Kcal/mol) that indicated favorable interactions and tight binding with the key amino acid residues at active site of tyrosinase. The His61, His259, His296, His244, Asn260 and Glu256 of tyrosinase were the sites for hydrogen bonding interactions with compound IIId. The docked conformation revealed that NO<sub>2</sub> group of compound IIId, which resided 2.25-2.27 Å adjacent to the di-copper nucleus, could form metal-ligand interaction (Figure 5D).

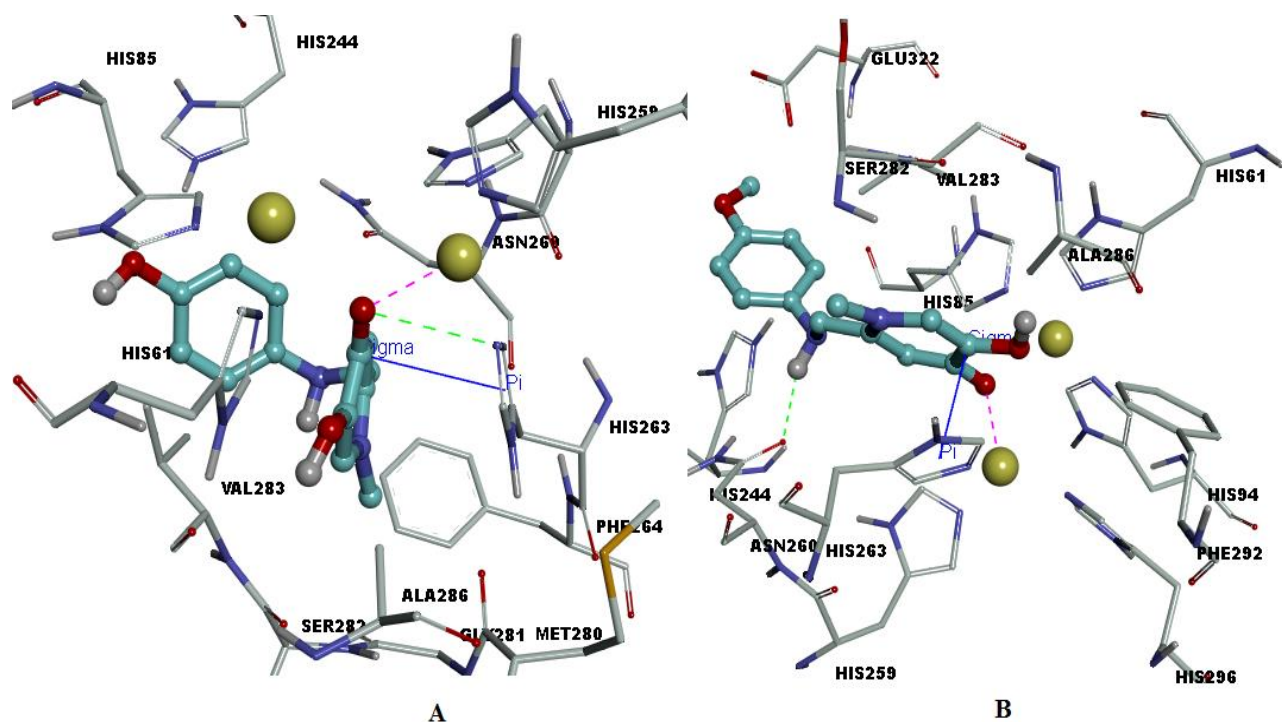
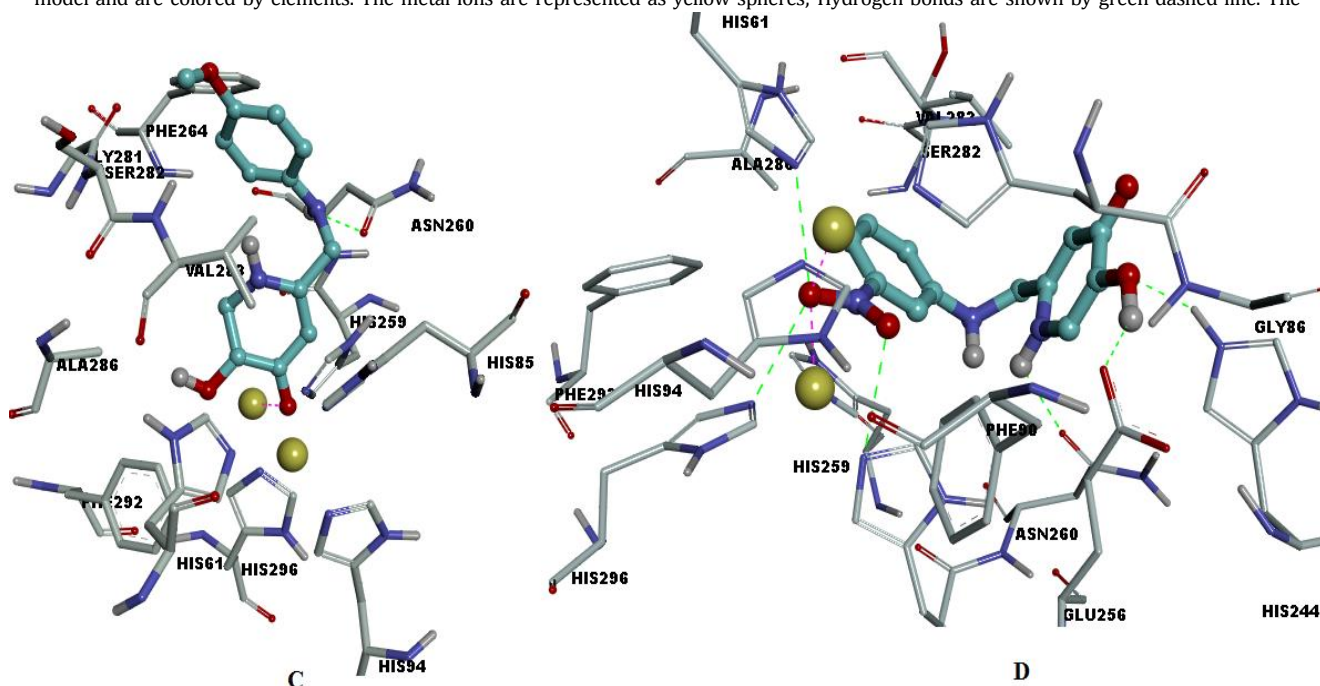


**Figure 5.** Binding model of compounds IIIa-d for the best docked pose in the tyrosinase active site. Ligands are represented by a ball and stick model and are colored by elements. The metal ions are represented as yellow spheres; Hydrogen bonds are shown by green dashed line. The



possible interaction between metal ions and ligands are marked by violet dashed line and Pi interactions represented as blue lines

Kojic acid derivatives IIIa-d were prepared in 89-94% yield by condensing 5-(benzyloxy)-1-methyl-4-oxo-1,4-dihydropyridine-2-carbaldehyde (**Ia**) and 5-(benzyloxy)-4-oxo-1,4-dihydropyridine-2-carbaldehyde (**Ib**), with appropriately substituted aniline in refluxing ethanol followed by the catalytic hydrogenation of the intermediates **IIa-d** over Pd/C as a catalyst. This

reaction resulted in the deprotection of the benzylated 5-hydroxy group and at the same time, the reduction of the C=N to a C-N bond for all compounds.

All compounds clearly showed a concentration-dependent inhibition against tyrosinase activity. Moreover, the inhibitory effect of compound **IIIId**, which has a nitro group substituent at the aromatic ring, on

tyrosinase activity was better than kojic acid. It appears that the tyrosinase inhibitory potency of the studied compounds to be in the order of **IIIId** > **KA** > **IIIa** > **IIIb** > **IIIc**. By comparing the IC<sub>50</sub>s of compounds **IIIa** and **IIIb** it may be suggested that the free hydroxyl group at the *para* position of the phenyl ring in compound **IIIa** seems to be important for the inhibition of the tyrosinase activity.

Compound **IIIb** has been found to be more active than **IIIc**. We have previously shown that the presence of a methyl group substituted at N-1 position of the hydroxypyridinone ring enhances the tyrosinase inhibitory activity. It was postulated that the inductive effect of this methyl group probably pushes more electrons to the oxygen atom of the C-4 carbonyl moiety making it a better ligand for the metal-ligand interaction in the tyrosinase active site (23).

The four prepared compounds were subjected to antioxidant evaluations. DPPH assay was carried out to evaluate the free radical scavenging activity of compounds. Methanolic solution of DPPH has a deep purple color and shows a strong absorption at 517 nm. If a compound possesses antioxidant activity, this color generally disappears when it is added to the DPPH solution. DPPH radical can accept an electron or hydrogen radical to become a stable bleached product (39). The inhibitory potency of compounds was in the order of **IIIc** > **IIIId** > **IIIa** > **IIIb** > **BHT**.

The results show that compounds with methyl substituent at N-1 atom of the pyridinone ring (**IIIa** and **IIIb**) exhibited less scavenging effects on DPPH radicals compared with compounds having no substituent on this atom (compounds **IIIc** and **IIIId**). It can be postulated that the labile hydrogen attached to the nitrogen atom can take part in the radical scavenging reaction and the resulted radical is stabilized by resonance with the alkene and carbonyl double bonds. The comparison of **IIIa** and **IIIc** structures shows that the NH moiety might be more effective in radical scavenging than the phenolic OH group. This can be confirmed by comparing compounds **IIIa** and **IIIId**.

Hydrogen peroxide itself is not very reactive, but it can cross cellular membranes and may oxidize a number of compounds such as essential thiol groups of proteins. H<sub>2</sub>O<sub>2</sub> inside the cell reacts with Fe<sup>2+</sup> and Cu<sup>2+</sup> to form OH• which is a highly reactive radical and exerts several toxic effects on the cell. Therefore, it is essential to control the amount of hydrogen peroxide to prevent oxidative stress conditions (40-41).

## Conclusion

In this research a combination of molecular docking approach and experimental evaluation of the tyrosinase inhibitory activity of some novel Kojic acid derivatives is reported. The antioxidant ability of these compounds is also described. Based on the molecular docking simulation studies, one of the studied compounds;

namely compound **IIIId**, was supposed to have the highest inhibitory activity amongst the studied compounds. This was also confirmed by tyrosinase activity inhibition assay. Compound **IIIId** has an NO<sub>2</sub> group which binds to both of Cu<sup>2+</sup> ions located inside the active site. This compound seems to be even more active than kojic acid in tyrosinase activity inhibition assay. In the docking experiments, all compounds were able to interact in a manner similar to the known inhibitors with the metal ions and residues located in the catalytic pocket of the enzyme. In all derivatives except **IIIId**, both the experimental inhibitory activity and the docking ΔG<sub>bind</sub> values were lower than KA. The DPPH free radical scavenging ability of the four studied compounds was more than that of BHT. However, they were not as strong as BHT or gallic acid in scavenging hydrogen peroxide.

Synthesis of more derivatives of the pyridinone scaffold as anti-tyrosinase compounds is underway in our research group. In the design of these compounds, the positive role of the nitro group in the inhibition of this enzyme or introducing more chelating moieties to the molecule for strong interaction with the di-copper nucleus are considered.

## Acknowledgment

The authors wish to send their gratitude to all members of Isfahan Pharmaceutical Sciences Research Center for their support and encouragement.

## References

1. Chang TS. An updated review of tyrosinase inhibitors. *Int J Mol Sci* 2009; 10:2440-2475.
2. Muñoz-Muñoz JL, García-Molina Mdel M, García-Molina F, Berna J, García-Ruiz PA, García-Moreno M, et al. Catalysis and inactivation of tyrosinase in its action on *o*-diphenols, *o*-aminophenols and *o*-phenylenediamines: Potential use in industrial applications. *J Mol Catal B Enzym* 2013; 91:17-24.
3. Therdphapiyanak N, Jaturanpinyo M, Waranuch N, Kongkanermit L, Sarisuta N. Development and assessment of tyrosinase inhibitory activity of liposomes of *Asparagus racemosus* extracts. *Asian J Pharm Sci* 2013; 8:134-142.
4. Li ZC, Chen LH, Yu XJ, Hu YH, Song KK, Zhou XW, et al. Inhibition kinetics of chlorobenzaldehyde thiosemicarbazones on mushroom tyrosinase. *J Agric Food Chem* 2010; 58:12537-12540.
5. Guerrero A, Rosell G. Biorational approaches for insect control by enzymatic inhibition. *Curr Med Chem* 2005; 12:461-469.
6. Loizzo MR, Tundis R, Menichini F. Natural and synthetic tyrosinase inhibitors as antibrowning agents: An update. *Compr Rev Food Sci Food Saf* 2012; 11:378-398.
7. Decker H, Schweikardt T, Nillius D, Salzbrunn U, Jaenicke E, Tuzcek F. Similar enzyme activation and catalysis in hemocyanins and tyrosinases. *Gene* 2007; 398:183-191.

8. De Faria RO, Moure VR, Lopes MA, Krieger N, Mitchell DA. The biotechnological potential of mushroom tyrosinases. *Food Technol Biotech* 2007; 45:287-294.
9. Aytemir MD, Karakaya G, Ekinci D. Kojic acid derivatives. In: Ekinci Deniz., editor. *Medicinal Chemistry and Drug Design*. 2012. pp. 1–26.
10. Noh JM, Kwak SY, Seo HS, Seo JH, Kim BG, Lee YS. Kojic acid–amino acid conjugates as tyrosinase inhibitors. *Bioorg Med Chem Lett* 2009; 19:5586-5589.
11. Burdock GA, Soni MG, Carabin IG. Evaluation of health aspects of kojic acid in food. *Regul Toxicol Pharmacol* 2001; 33:80-101.
12. Rho HS, Lee CS, Ahn SM, Hong YD, Shin SS, Park YH, et al. Studies on tyrosinase inhibitory and antioxidant activities of benzoic acid derivatives containing kojic acid moiety. *Bull Korean Chem Soc* 2011; 32:4411-4414.
13. Rho HS, Ahn SM, Yoo DS, Kim MK, Cho DH, Cho JY. Kojyl thioether derivatives having both tyrosinase inhibitory and anti-inflammatory properties. *Bioorg Med Chem Lett* 2010; 20:6569–6571.
14. Noh JM, Kwak SY, Kim DH, Lee YS. Kojic acid–tripeptide amide as a new tyrosinase inhibitor. *Biopolymers* 2007; 88:300-307.
15. Lee YS, Park JH, Kim MH, Seo SH, Kim HJ. Synthesis of tyrosinase inhibitory kojic acid derivatives. *Arch Pharm Chem Life Sci* 2006; 339:111-114.
16. Wempe M, Fitzpatrick M. 5-Hydroxy-2-methyl-4H-pyran-4-one-esters as novel tyrosinase inhibitors, WO 2009/108271 A1.
17. Mohammadpour M, Behjati M, Sadeghi A, Fassihi A. Wound healing by topical application of antioxidant iron chelators: kojic acid and deferiprone. *Int Wound J* 2012; 10:260-264.
18. Mohammadpour M, Sadeghi A, Fassihi A, Saghaei L, Movahedian A, Rostami M. Synthesis and antioxidant evaluation of some novel orthohydroxypyridine-4-one iron chelators. *Res Pharm Sci* 2012; 3:171-179
19. Ahn SM, Rho HS, Baek HS, Joo YH, Hong YD, Shin SS, et al. Inhibitory activity of novel kojic acid derivative containing trolox moiety on melanogenesis. *Bioorg Med Chem Lett* 2011; 24:7466-7469.
20. Lajis AF, Hamid M, Ariff AB. Depigmenting effect of kojic acid esters in hyperpigmented B16F1 melanoma cells. *J Biomed Biotechnol* 2012; 1-9.
21. Huang SY, Zou X. Advances and challenges in protein-ligand docking. *Int J Mol Sci* 2010; 11:3016–3034.
22. Mukesh B, Rakesh K. Molecular docking: A review. *Int J Res Ayurveda Pharm* 2011; 2:746–1751.
23. Saghaie L, Pourfarzam M, Fassihi A, Sartippour B. Synthesis and tyrosinase inhibitory properties of some novel derivatives of kojic acid. *Res Pharm Sci* 2013; 8:233-242.
24. Morris GM, Huey R, Lindstrom W, Sanner MF, Belew RK, Goodsell DS, et al. AutoDock4 and AutoDockTools4: Auto-mated docking with selective receptor flexibility. *J Comput Chem* 2009; 30:2785-2791.
25. Morris GM, Goodsell DS, Halliday RS, Huey R, Hart WE, Belew RK, et al. Automated docking using a Lamarckian genetic algorithm and an empirical binding free energy function. *J Comput Chem* 1998; 19:1639-1662.
26. Gasteiger J, Marsili M. Iterative partial equalization of orbital electronegativity—a rapid access to atomic charges. *Tetrahedron* 1980; 36:3219-322
27. Ismaya WT, Rozeboom HJ, Weijn A, Mes JJ, Fusetti F, Wichers HJ, et al. Crystal structure of *Agaricus bisporus* mushroom tyrosinase: Identity of the tetramer subunits and interaction with tropolone. *Biochemistry* 2011; 50:5477-5486.
28. Discovery Studio Visualizer. Release 3.5, Accelrys Software Inc., San Diego CA USA, 2012.
29. Weiner SJ, Kollman PA, Case DA, Singh UC, Ghio C, Alagona G, et al. A new force field for molecular mechanical simulation of nucleic acids and proteins. *J Am Chem Soc* 1984; 106:765-784.
30. Wallace AC, Laskowski RA, Thornton JM . LIGPLOT: A program to generate schematic diagrams of protein-ligand interactions. *Protein Eng* 1995; 8:127-134.
31. Iida K, Hase K, Shimomura K, Sudo S, Kadota S, Namba T. Potent inhibitors of tyrosinase activity and melanin biosynthesis from *Rheum officinale*. *Planta Med* 1995; 161:425-428.
32. Blois MS. Antioxidant determinations by the use of a stable free radical. *Nature* 1958; 181:1199-1200
33. Ruch RJ, Cheng SJ, Klaunig JE. Prevention of cytotoxicity and inhibition of intracellular communication by antioxidant catechins isolated from Chinese green tea. *Carcinogenesis* 1989; 10:1003-1008.
34. Wen KC, Chang CS, Chien YC, Wang HW, Wu WC, Wu CS, et al. Tyrosol and its analogues inhibit alpha-melanocyte-stimulating hormone induced melanogenesis. *Int J Mol Sci* 2013; 14:23420-23440.
35. Vontzalidou A, Zoidis G, Chaita E, Makropoulou M, Aliogiannis N, Lambrinidis G, et al. Design, synthesis and molecular simulation studies of dihydrostilbene derivatives as potent tyrosinase inhibitors. *Bioorg Med Chem Lett* 2012; 22:5523–5526.
36. Chung KW, Jeong HO, Jang EJ, Choi YJ, Kim DH, Kim SR, et al. Characterization of a small molecule inhibitor of melanogenesis that inhibits tyrosinase activity and scavenges nitric oxide (NO). *Biochim Biophys Acta* 2013; 1830:4752–4761.
37. Pei CJ, Lee J, Si YX, Oh S, Xu WA, Yin SJ, et al. Inhibition of tyrosinase by gastrodin: An integrated kinetic-computational simulation analysis. *Proc Biochem* 2013; 48:162–168.
38. Wang Z, Lee J, Si YX, Oh S, Yang JM, Shen D, et al. Toward the inhibitory effect of acetylsalicylic acid on tyrosinase: Integrating kinetics studies and computational simulations. *Proc Biochem* 2013; 48:260–266.
39. Ferreira ICFR, Baptista P, Vilas-Boas M, Barros L. Free-radical scavenging capacity and reducing power of wild edible mushrooms from northeast Portugal:

Individual cap and stipe activity. Food Chem 2007; 100:1511–1516.

40. Halliwell B, Gutteridge JMC. Free Radicals in Biology and Medicine. 4<sup>th</sup> ed. Oxford, UK: Clarendon Press; 2006.

41. Pise NM, Jena KB, Maharana D, Sabale AB, Jagtap TG. Free radical scavenging, reducing power, phenolic and biochemical composition of *Porphyra* species. J Algal Biomass Utiln 2010; 1:60-73.